LHCb-PUB-2019-013
September 10, 2019

Upgrade trigger selection studies

Alejandro Alfonso Albero[1], Varvara Batozskaya[2], Sean Benson[3], Mikkel Bjørn[4], Steve Blusk[5], Veronika Chobanova[6], Greg Ciezarek[7], Agnieszka Dziurda[8], Conor Fitzpatrick[7], Ekaterina Govorkova[3], Kevin Heinicke[9], Donal Hill[4], Nathan Jurik[4], Xuesong Liu[10], Olli Lupton[7], Patrick Mackowiak[9], Carla Marin Benito[11], Diego Martínez Santos[6], Marcel Materok[12], Rosen Matev[7], Antje Modden[9], Vanessa Müller[9], Alex Pearce[7], Miguel Ramos Pernas[6], Nicola Skidmore[13], Eluned Smith[12], Sascha Stahl[7], Ricardo Vazquez Gomez[7], Mengzhen Wang[10], Mark Whitehead[12], Constantin Weisser[14], Ao Xu[10], Lauren Yeomans[15]

[1] *Universitat de Barcelona,* [2] *National Centre for Nuclear Research (NCBJ), Warsaw, Poland,* [3] *Nikhef Amsterdam,* [4] *University of Oxford,* [5] *Syracuse University,* [6] *IGFAE,* [7] *CERN,* [8] *Henryk Niewodniczanski Institute of Nuclear Physics (PAN),* [9] *Dortmund,* [10] *Tsinghua University,* [11] *LAL Orsay,* [12] *RWTH Aachen University,* [13] *Ruprecht-Karls-Universität Heidelberg,* [14] *Massachusetts Institute of Technology,* [15] *University of Liverpool*

Abstract

This document describes the selection strategies for the upgrade trigger using a range of decay channels that are representative of the current, and planned, physics programme. The upgrade high-level trigger (HLT) follows the Run 2 trigger structure consisting of two stages, in between which the detector calibration and alignment is performed. In the first stage, HLT1, beauty and charm decays are selected inclusively, while the second stage, HLT2, uses offline-quality selections. Inclusive and exclusive trigger selections in HLT2 are presented, and the output rates, signal efficiencies, event sizes and bandwidth usage are discussed.

Contents

1 Introduction

The LHCb detector will be upgraded between 2019–2021, during the second long shutdown of the LHC. The objective of this upgrade is to allow the LHCb detector to take data at an instantaneous luminosity of 2×10^{33} cm^{-2}s^{-1}, a factor of five more than during LHC Run 2. A key requirement is to process the full 30 MHz bunch crossing rate of the LHC using a dedicated computing centre. This software only approach, as shown in Fig. 1 (right), requires two stages: a fast reconstruction and selection stage referred to as HLT1, and a second step with full reconstruction and real-time analysis known as HLT2. Between the two trigger stages the real-time alignment and calibration of the detector are performed. The main difference with respect to the Run 2 scheme, which is depicted in Fig. 1 (left), is the removal of the L0 hardware trigger. More details of the objectives and strategy are given in the LHCb upgrade framework TDR [1], the Trigger TDR [2] and the Computing Model of the Upgrade LHCb experiment TDR [3].

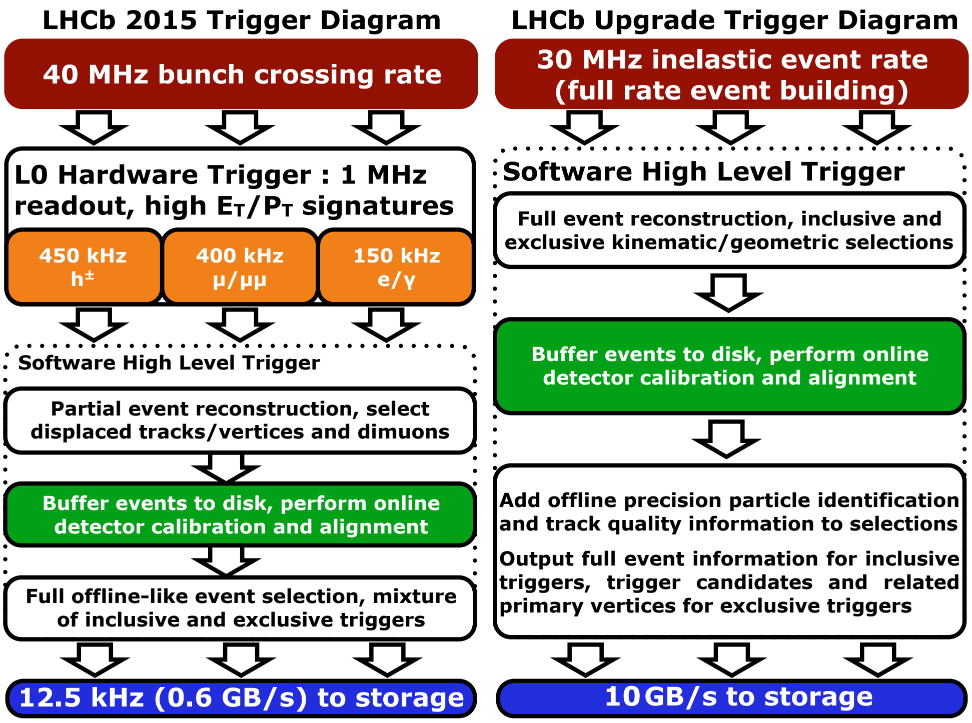

Figure 1: Trigger strategy for (left) LHCb Run 2 and (right) the LHCb upgrade project, assuming a total 10 GB/s output bandwidth.

It is expected that an inclusive topological B trigger (see Section 4.7 for details) will be fully utilised during the first year of data taking in 2021 [3]. This is motivated by the need to be able to develop new analyses using the data collected in 2021 and to study the application of important tools, such as flavour-tagging, that currently require full event information, in the Turbo stream [4, 5]. The Turbo stream was implemented for LHCb Run 2, providing data samples that can be analysed directly from the trigger output, without further processing. As analyses mature, exclusive selections will be implemented in HLT2, taking advantage of the Turbo paradigm to dramatically reduce the event size and therefore the trigger bandwidth required. This will be a necessary step to control the trigger bandwidth as the experiment is commissioned to its full design luminosity.

This document is focused on the event selection, in particular at the HLT2 stage. The goals of these studies are

1. to study the signal efficiencies, rates and bandwidth used by exclusive and inclusive trigger selections;
2. to understand the effect of different HLT1 strategies on the selection efficiencies of physics channels in HLT2;
3. to perform a feasibility study of inclusive triggers in the upgrade era;
4. to demonstrate the gains from using multi-variate selections in the trigger;
5. to understand the event size needed for each trigger selection.

A baseline of four configurations at the HLT1 stage are considered, as described in Section 3. The physics selection studies for HLT2 are shown in Section 4, where the performance in terms of signal efficiency, rate and output bandwidth per selection are shown. This work builds on the studies shown for a selection of charm decays discussed in Ref. [6]. A conclusion completes the document in Section 5.

2 Data samples

The studies presented in this document are based on simulated samples of pp collisions, at $\sqrt{s} = 14$ TeV, including the upgrade detector geometry and beam conditions.[1] The collisions are generated using Pythia [7] with a specific LHCb configuration [8]. Decays of hadronic particles are described by EvtGen [9], in which final-state radiation is generated using Photos [10]. The interaction of the generated particles with the detector, and its response, are implemented using the Geant4 toolkit [11] as described in Ref. [12]. The samples are reconstructed using the upgrade tracking sequence that is described in Ref. [13], and then filtered using the `VLoose` HLT1 trigger requirements described in Section 3. The HLT1 filtering rejects 95% of minimum bias events, with signal efficiencies for the exclusive decays considered in the present study ranging between 50–90%. A sample of roughly 50M minimum bias events is used to study the output rates and bandwidth of each physics selection. Roughly thirty signal samples, of approximately 250k events each, are generated for the purpose of evaluating the signal efficiencies.

3 First stage: HLT1

The HLT1 configuration used to filter the various samples generated for these studies contains inclusive selections for single displaced tracks, displaced two-track vertices, single displaced muons, and displaced low-mass dimuon vertices and high-mass dimuon candidates. This configuration includes various working points for each selection, and the four scenarios `VLoose`, `Loose`, `Tight`, `VTight` are defined by taking different combinations of these selections. The effect of these different HLT1 scenarios on subsequent selections in HLT2 is explored in Section 4, with a particular focus on the HLT1-dependence of the signal efficiencies.

[1]The specific simulated conditions are Sim09c-Up02/Reco-Up01 with 7 TeV beam energies, spillover included, 25 ns bunch spacing and $\nu = 7.6$ using Pythia 8.

The final choice of HLT1 configuration may be restricted by software performance and attainable throughput, but these studies will provide important input to ensure that any performance-related compromises have the smallest possible impact on the upgrade physics programme.

The HLT1 configuration used to filter the various samples in this study is defined in the trigger configuration key TCK `0x52000000`, which is compatible with `v30r0` of the LHCb trigger application, Moore. A number of different options are included in the configuration: four options from `VLoose` to `VTight` for the one-track MVA line `Hlt1TrackMVA`; similarly four choices for the two-track MVA line `Hlt1TwoTrackMVA`; two selections, loose and tight, for each of the low and high mass dimuon lines `Hlt1DiMuonLowMass` and `Hlt1DiMuonHighMass` (labelled `Hlt1DiMuon` together); and a single option for the one-track muon MVA line `Hlt1TrackMuonMVA`. The combinations of these selections that form the four considered scenarios are given in Table 1.

A global event cut (GEC), which aborts processing of events with more than 11500 clusters from the UT and SciFi detectors, is imposed for all selections except for the `VLoose` `Hlt1TrackMVA` and `Loose Hlt1DiMuon` cases. The GEC requirements reject approximately 10% of minimum bias candidates when applied to the different HLT1 scenarios. This requirement will be tuned in the future by also considering the signal efficiencies for a range of decay topologies.

The configurations of the one- and two-track `TrackMVA` selections are taken from Ref. [6], which defines “loose” and “tight” configurations of both selections. The `VLoose` and `Loose` selections use the “loose” `TrackMVA` tunings, for both one- and two-track lines, described in Ref. [6], while `Tight` and `VTight` use the “tight” tunings. Due to the stringent throughput requirements that HLT1 must meet, it is currently unclear what low-p_{T} tracking will be available up-front. Given this, the different `TrackMVA` selections simulate different p_{T} tracking thresholds. The `VLoose` selections assume tracks are available down to a p_{T} of $400\,\mathrm{MeV}/c$, the `Loose` and `Tight` selections simulate a p_{T} threshold of $800\,\mathrm{MeV}/c$, while the `VTight` selections require $p_{\mathrm{T}} > 1400\,\mathrm{MeV}/c$.

The `Hlt1TrackMuonMVA` selection is similar to the selection of the same name that has been used during Run 2; it is, in essence, a looser version of the `VLoose Hlt1TrackMVA` line that additionally imposes muon identification criteria.

The `Hlt1DiMuon` selections are also based on selections used during Run 2. The `Hlt1DiMuonLowMass` variants require that both muons have $p_{\mathrm{T}} > 800\,\mathrm{MeV}/c$ and are displaced from all primary vertices, while the `Hlt1DiMuonHighMass` selections omit the displacement requirement but instead require a dimuon mass of $> 2.7\,\mathrm{GeV}/c^2$. The loose and tight variants differ by a stricter p_{T} threshold of $1400\,\mathrm{MeV}/c$ for the tight case.

The output rates of the HLT1 selections are 1.65 ± 0.03 (`VLoose`), 1.10 ± 0.03 (`Loose`), 0.48 ± 0.02 (`Tight`) and 0.29 ± 0.01 MHz (`VTight`). These cover a range of realistic throughput scenarios for HLT1, given by the different tracking p_{T} thresholds described above. The final choice between them will depend on both the trigger performance and the size of the available computing farm.

4 Second stage: HLT2

The selections in HLT2 must fit into an estimated total output bandwidth of between 2 and 10 GB/s, where the final choice will be informed by the available offline computing

Table 1: Definition of the four HLT1 scenarios including the minimum track p_T requirement and the output rate.

Scenario	Hlt1TrackMVA	Hlt1DiMuon	Hlt1TrackMuonMVA	Min. track p_T (MeV/c)	Rate (MHz)
VLoose	VLoose	Loose	Yes	400	1.65
Loose	Loose	Tight	Yes	800	1.10
Tight	Tight	Tight	Yes	800	0.48
VTight	VTight	Tight	No	1400	0.29

resources. Both exclusive and inclusive approaches are studied, with particular attention given to reducing the size of each event by saving only the necessary information, following the Turbo stream paradigm [4].

The HLT2 efficiencies described in this section, are defined relative to the `VLoose` HLT1 stage using reconstructible, truth-matched events. To be considered reconstructible, events must have all charged decay product tracks within the detector acceptance. Neutral decay products are required to be within the electromagnetic calorimeter acceptance. The relative efficiency of the HLT2 selections under the different HLT1 options are also studied. A candidate is labelled as *TOS*, with respect to an HLT1 selection, if its own decay products satisfy the requirements of that selection. A relative efficiency is then defined, with respect to the number of candidates selected by HLT2, as the ratio of the number of candidates that are TOS in a given HLT1 scenario to the number of candidates in which any particle(s) in the event satisfies the `VLoose` HLT1 requirements. These studies show clearly how the signal efficiencies scale with tighter HLT1 requirements.

Expected signal rates are determined for each signal decay process. These are based on the instantaneous luminosity, the measured cross-sections for particles to be produced within the LHCb acceptance, and the branching ratio of the decay of interest. Note that often the same trigger line is also used to select control modes that typically have a significantly higher rate. Therefore it is not expected that even a perfect exclusive selection has an output rate equal to the expected signal rate.

The selections are described below, grouped primarily by the LHCb physics working group responsible.

4.1 Charm

Approximately 160 exclusive charm trigger lines have been implemented in the Turbo paradigm in Run 2 of the LHCb experiment. The first step to study the upgrade selections is to test the performance of the Run 2 Turbo stream selections in the upgrade environment. Nine decay modes are considered here, as listed in Table 2. The selections used during Run 2 are applied to the HLT1 filtered simulation samples for both signal and minimum bias events. Reconstruction of K^0_S at LHCb is split into two categories, those reconstructed from tracks with (LL) and without (DD) hits in the LHCb vertex locator. Only those of type LL are consider for charm decays at this stage.

The signal efficiencies of the HLT2 selections for the nine modes are shown in Table 2. The relative efficiencies of the various HLT1 scenarios are shown in Table 3, calculated as the fraction of events passing each selection relative to the `VLoose` criterion. The entries in the first column are not 100% because the trigger decision is required to be from one of

Table 2: Signal efficiency, output rate, expected signal-only rate, event size and bandwidth of the HLT2 charm selections for the `VLoose` HLT1 scenario.

Decay mode	Efficiency (%)	Rate (Hz)	Sig. rate (Hz)	Event size (kB)	Bandwidth (kB/s)
$D^{*+} \to D^0(\to K^+K^-)\pi^+$	50	800	1100	6	4800
$D^{*+} \to D^0(\to K^+K^-\pi^+\pi^-)\pi^+$	28	650	310	7	4500
$D^{*+} \to D^0(\to K^0_S\pi^+\pi^-)\pi^+$	19	290	770	7	7700
$D^{*+} \to D^0(\to K^0_S K^+K^-)\pi^+$	14	35	120	7	840
$D^+ \to K^-K^+\pi^+$	49	2700	4800	6	16000
$\Lambda_c^+ \to pK^-\pi^+$	21	5400	11000	6	32000
$D^{*+} \to D^0(\to \pi^+\pi^-\mu^+\mu^-)\pi^+$	38	46	0.2	7	320
$D^{*+} \to D^0(\to e^+\mu^-)\pi^+$	60	220	< 0.1	4	880
$\Xi_{cc}^{++} \to \Lambda_c^+(\to pK^-\pi^+)K^-\pi^+\pi^+$	4	23	0.2	6	140

Table 3: Relative efficiency of the HLT2 selections given the different HLT1 scenarios for the charm decay modes. The relative efficiency is defined as the ratio of the number of candidates that are TOS in a given HLT1 scenario to the number of candidates in which any particle(s) in the event satisfies the `VLoose` HLT1 requirements.

Decay mode	`VLoose` (%)	`Loose` (%)	`Tight` (%)	`VTight` (%)
$D^{*+} \to D^0(\to K^+K^-)\pi^+$	96	90	66	47
$D^{*+} \to D^0(\to K^+K^-\pi^+\pi^-)\pi^+$	89	74	46	30
$D^{*+} \to D^0(\to K^0_S\pi^+\pi^-)\pi^+$	81	64	36	21
$D^{*+} \to D^0(\to K^0_S K^+K^-)\pi^+$	76	66	34	20
$D^+ \to K^-K^+\pi^+$	97	84	69	42
$\Lambda_c^+ \to pK^-\pi^+$	95	82	55	41
$D^{*+} \to D^0(\to \pi^+\pi^-\mu^+\mu^-)\pi^+$	96	77	56	42
$D^{*+} \to D^0(\to e^+\mu^-)\pi^+$	90	80	58	40
$\Xi_{cc}^{++} \to \Lambda_c^+(\to pK^-\pi^+)K^-\pi^+\pi^+$	95	83	62	47

the particles of the signal decay, relative to the `VLoose` criterion satisfied by any particle in the event. Figure 2 shows the rate against the signal efficiency for the nine decay modes. This highlights the large losses in signal efficiency from applying the stricter HLT1 requirements.

The average event size of the different decay modes ranges from 4 kB to 7 kB, as shown in Table 2. The bandwidths for the selections are also shown in Table 2 and range from 140 to 32000 kB/s.

During Run 2, the trigger lines for the modes studied here represented around 6% of the charm bandwidth in the Turbo stream. Extrapolating the charm bandwidth of roughly 65 MB/s in Table 2 by this factor of 6% gives a total charm upgrade Turbo stream bandwidth of order 1 GB/s. This is a large part of the available HLT2 output bandwidth; however, no multivariate techniques have been applied here. These methods will be studied in the future to reduce the rate of the lines further without sacrificing much signal efficiency. Multivariate approaches appear to be particularly necessary for the high-rate lines for $D^+ \to K^-K^+\pi^+$ and $\Lambda_c^+ \to pK^-\pi^+$ decays.

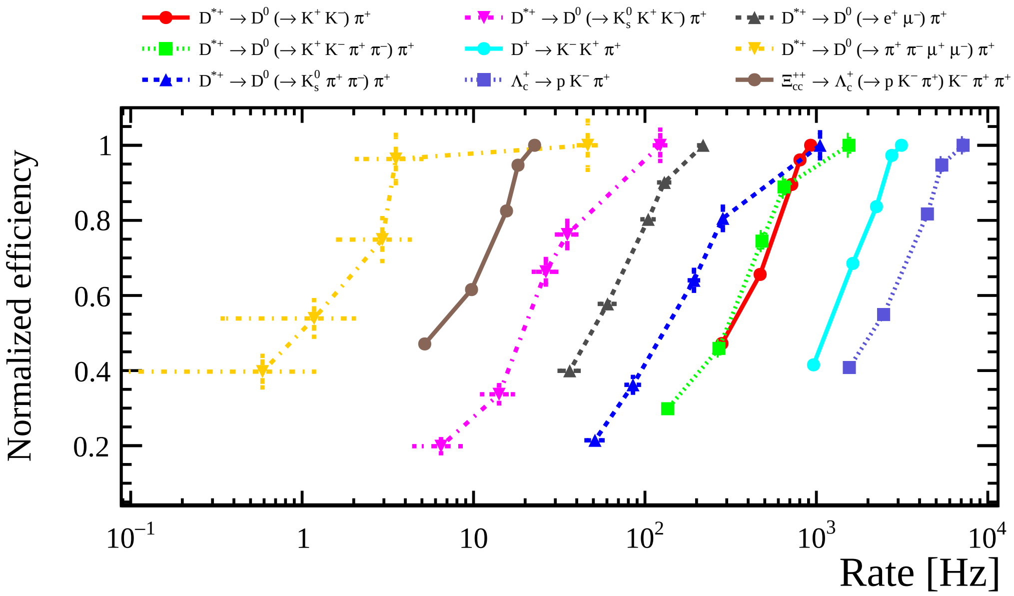

Figure 2: The relative signal efficiency (see Table 3) as a function of the output rate for different modes and different HLT1 scenarios.

Table 4: Signal efficiency, output rate, expected signal-only rate, event size and bandwidth of the HLT2 beauty to open charm selections for the `VLoose` HLT1 scenario.

Decay mode	Efficiency (%)	Rate (Hz)	Sig. rate (Hz)	Event size (kB)	Bandwidth (kB/s)
$B^+ \to D^0(\to K^0_S\pi^+\pi^-)K^+$	20	42	0.2	6	250
$B^0 \to D^+(\to K\pi\pi)D^-(\to K\pi\pi)$	18	10	0.1	16	160
$B^+ \to D^0(\to K^+K^-)K^+$	22	7	0.1	4	28
$B^0_s \to D^+_s(\to KK\pi)K^-$	32	290	0.2	14	4100
$B^+ \to D^0(\to K\pi)K^+\pi^+\pi^-$	17	170	0.9	7	1200

4.2 Beauty to open charm

The following five representative decay modes are studied: $B^+ \to D^0(\to K^0_S\pi^+\pi^-)K^+$, $B^0_s \to D^+_s(\to KK\pi)\pi^-$, $B^0 \to D^+(\to K\pi\pi)D^-(\to K\pi\pi)$, $B^+ \to D^0(\to K^+K^-)K^+$ and $B^+ \to D^0(\to K\pi)K^+\pi^+\pi^-$. Note that results for the $B^+ \to D^0(\to K^0_S\pi^+\pi^-)K^+$ channel are later split into two components, depending on the reconstruction of the K^0_S mesons. The starting point for the upgrade selections is the current Run 2 preselections that are performed offline with some small tuning and adjustments to make them more efficient and consistent. The selections applied are summarised in the Appendix in Table 19. Particle identification requirements are not always applied because often the control decay modes, used to reduce systematic uncertainties, only differ from the signal decays by the species of one particle.

The average event sizes are listed in Table 4 for each of the modes. For $B^0 \to D^+(\to K\pi\pi)D^-(\to K\pi\pi)$ and $B^0_s \to D^+_s(\to KK\pi)K^-$ decays, the information required for flavour tagging is additionally saved which increases the event size by $\mathcal{O}(10)$ kB. The output rates and relative signal efficiencies used by each decay mode are studied for each

Table 5: Rates of the HLT2 selections given the different HLT1 scenarios for the beauty to open charm decay modes.

Decay mode	`VLoose` (Hz)	`Loose` (Hz)	`Tight` (Hz)	`VTight` (Hz)
$B^+ \to D^0(\to K^0_S\pi^+\pi^-)K^+$	42	23	6	4
K^0_S (DD)	33	18	5	3
K^0_S (LL)	10	5	1	1
$B^0 \to D^+(\to K\pi\pi)D^-(\to K\pi\pi)$	10	6	2	1
$B^+ \to D^0(\to K^+K^-)K^+$	7	4	1	1
$B^0_s \to D^+_s(\to KK\pi)K^-$	290	140	28	14
$B^+ \to D^0(\to K\pi)K^+\pi^+\pi^-$	170	83	22	13

Table 6: Relative efficiency of the HLT2 selections given the different HLT1 scenarios for the beauty to open charm decay modes. The relative efficiency is defined as the ratio of the number of candidates that are TOS in a given HLT1 scenario to the number of candidates in which any particle(s) in the event satisfies the `VLoose` HLT1 requirements.

Decay mode	`VLoose` (%)	`Loose` (%)	`Tight` (%)	`VTight` (%)
$B^+ \to D^0(\to K^0_S\pi^+\pi^-)K^+$	95	90	81	71
K^0_S (DD)	93	87	80	67
K^0_S (LL)	100	100	83	83
$B^0 \to D^+(\to K\pi\pi)D^-(\to K\pi\pi)$	100	90	87	73
$B^+ \to D^0(\to K^+K^-)K^+$	99	92	87	82
$B^0_s \to D^+_s(\to KK\pi)K^-$	99	91	85	75
$B^+ \to D^0(\to K\pi)K^+\pi^+\pi^-$	100	91	88	79

of the HLT1 scenarios. Table 5 shows the results of the rate studies. The signal efficiencies are shown in Table 4 for the nominal results, and Table 6 shows the results of these studies for each of the HLT1 scenarios.

The output bandwidth required for the five decay modes is summarised in Table 4. The bandwidth required in the `VLoose` HLT1 scenario for the $B^0_s \to D^+_s(\to KK\pi)K^-$ and $B^+ \to D^0(\to K\pi)K^+\pi^+\pi^-$ lines is high, suggesting that more can be done to improve the performance. Given that these five modes are representative of the beauty to open charm programme, the total rate and bandwidth can be extrapolated by a factor of ten to estimate the total for all such decays. This gives a modest rate of 5.2 kHz and bandwidth of 45 MB/s.

The results in Tables 5 and 6 show that the minimum bias rates drop much faster than the signal efficiencies with tighter HLT1 selection requirements. This suggests that improvements can be made to the HLT2 selections to reduce the rates further without strongly impacting the signal efficiencies.

In parallel to further studies to improve the exclusive selections described above, it is interesting to understand the performance of the inclusive topological triggers (see Section 4.7) for these decays modes. However, the exclusive studies remain important because these selections will be required at some stage of the online or offline data flow.

Table 7: Signal efficiency, output rate, expected signal-only rate, event size and bandwidth of the HLT2 beauty to charmonia selections for the `VLoose` HLT1 scenario.

Decay mode	Efficiency (%)	Rate (Hz)	Sig. rate (Hz)	Event size (kB)	Bandwidth (kB/s)
$B^0 \to J/\psi\,(\to \mu^+\mu^-)\,K^0_S$	49	20	0.6	15	300
$B^0 \to J/\psi\,(\to \mu^+\mu^-)\,\rho^0$	29	21	0.1	5	110
$B^0_s \to J/\psi\,(\to e^+e^-)\,\phi$	5	76	1.5	15	1100
$B^0_s \to J/\psi\,(\to \mu^+\mu^-)\,\phi$	43	310	2.5	15	4700

Table 8: Relative efficiency of the HLT2 selections given the different HLT1 scenarios for the beauty to charmonia decay modes. The relative efficiency is defined as the ratio of the number of candidates that are TOS in a given HLT1 scenario to the number of candidates in which any particle(s) in the event satisfies the `VLoose` HLT1 requirements.

Decay mode	`VLoose` (%)	`Loose` (%)	`Tight` (%)	`VTight` (%)
$B^0 \to J/\psi\,(\to \mu^+\mu^-)\,K^0_S$	96	83	83	45
$B^0 \to J/\psi\,(\to \mu^+\mu^-)\,\rho^0$	94	80	80	46
$B^0_s \to J/\psi\,(\to e^+e^-)\,\phi$	95	84	62	46
$B^0_s \to J/\psi\,(\to \mu^+\mu^-)\,\phi$	95	81	81	45

4.3 Beauty to charmonia

The focus of this working group is to study decay modes with $c\bar{c}$ mesons in the final state. For the upgrade selection studies the following channels are considered; $B^0 \to J/\psi\,(\to \mu^+\mu^-)\,K^0_S(\to \pi^+\pi^-)$, $B^0 \to J/\psi\,(\to \mu^+\mu^-)\,\rho^0$, $B^0_s \to J/\psi\,(\to e^+e^-)\,\phi$ and $B^0_s \to J/\psi\,(\to \mu^+\mu^-)\,\phi$. For the $B^0 \to J/\psi\,K^0_S$ mode, both LL and DD categories for the K^0_S are considered together. The selection for each decay mode is based on the corresponding preselection used for LHCb Run 2 data with some additional tighter requirements applied. The cut values can be found in Tables 20, 21, 22 and 23 in the Appendix.

The signal efficiency, rate, event size and bandwidth for the different selections are shown in Table 7. The corresponding relative signal efficiencies in the different HLT1 scenarios, are given in Table 8, where a 50% drop in efficiency is seen between the `VLoose` and `VTight` options. The event size for $B^0 \to J/\psi\,\rho^0$ is smaller because it does not include flavour tagging information.

The initial selection for the $B^0_s \to J/\psi\,(\to e^+e^-)\,\phi$ channel was extremely loose, the rate for this channel estimated using the minimum bias sample was found to be 0.7 MHz. To improve it, a much tighter selection is used, leading to more realistic numbers for the rate. However, the selection is now rather tight with a low signal efficiency, so further study is required to check how feasible the current selection is in Run 3. Multivariate techniques will be studied for all of these modes in the future to reduce the bandwidth required whilst keeping the signal efficiencies as high as possible. In addition, improvements to the upgrade tunings of the electron particle identification variables are expected, these will help to improve the performance of the $B^0_s \to J/\psi\,(\to e^+e^-)\,\phi$ selection.

Table 9: Signal efficiency, output rate, expected signal-only rate, event size and bandwidth of the HLT2 $B^0_s \to \phi\phi$ selection for the `VLoose` HLT1 scenario.

Decay mode	Efficiency (%)	Rate (Hz)	Sig. rate (Hz)	Event size (kB)	Bandwidth (kB/s)
$B^0_s \to \phi\phi$	88	190	0.1	18	3400

4.4 Charmless beauty decays

The starting point for the upgrade selection of the $B^0_s \to \phi\phi$ decay is taken from the current requirements implemented in the final stage of the central productions during Run 2. The values are provided in Table 24 of the Appendix. Candidates passing the selection requirements described in Table 24 are then categorised by a neural network in the SciKit-Learn framework [14]. The neural network is trained using simulated signal and background samples as described in Section 2. The training samples are also required to pass the requirements listed in Table 24. The features of the decays used to train the network are the B^0_s impact parameter (IP) χ^2, B^0_s p_{T}, ϕ p_{T}, and the B^0_s vertex quality.

The chosen neural network requirement rejects 98 % of background candidates while retaining 95 % of the signal candidates. In order to make the classifier suitable for use in the LHCb production environment, the NNDrone package [15] is used, which converts the network model to a `JSON` format that can then be read by a dedicated algorithm in the software framework.

The event sizes (including the flavour tagging information) and overall efficiencies are given in Table 9. The output rate and event size from the minimum bias sample correspond to an output bandwidth of 3400 kB/s for the `VLoose` HLT1 requirements.

4.5 Beauty hadrons and quarkonia

4.5.1 Selection for excited Λ^0_b decays

The spectroscopy programme of LHCb requires the efficient selection of excited b-hadron decays where some of the decay products are typically consistent with originating from the primary vertex. In decays of longer lived b-hadrons, the decay vertex of the parent particle is significantly displaced from the primary vertex allowing for selection criteria based on the large impact parameter of the final state particles. The decay $\Lambda^{*0}_b \to \Lambda^0_b \pi^+\pi^-$ where $\Lambda^0_b \to \Lambda^+_c \pi^-$ and $\Lambda^+_c \to pK^-\pi^+$ is particularly challenging as these requirements cannot be used. To allow flexibility and extrapolation to other decay channels, the selection utilises selective persistence to save additional tracks from the same primary vertex as the b-hadron.

The selection requirements are presented in Table 25 in the Appendix. The results shown in Table 10 are based on the simulated sample of $\Lambda^{*0}_b \to \Lambda^0_b \pi^+\pi^-$ decays. The minimum bias retention is around 0.01%. This corresponds to an output rate of 3 kHz and an output bandwidth of 15 MB/s. The relative efficiency of the various HLT1 filtering configurations on the signal sample are given in Table 11. Future studies to reduce the rate will include the application of multivariate techniques and tuning of the requirements described above.

Table 10: Signal efficiency, output rate, expected signal-only rate, event size and bandwidth of the HLT2 beauty hadrons and quarkonia selections for the `VLoose` HLT1 scenario. *The total rate for the $H_b \to J/\psi X$ line is estimated at 0.62 kHz, with a signal rate of 0.14 kHz. **The output bandwidth for the $H_b \to J/\psi X$ line is 3100 kB/s.

Decay Mode	Efficiency (%)	Rate (Hz)	Sig. rate (Hz)	Event size (kB)	Bandwidth (kB/s)
$\Lambda_b^{*0} \to \Lambda_b^0 \pi^+\pi^-$	28	3000	0.2	5	15000
$B^0 \to J/\psi \rho$	20	*	0.1	5	**
$B^+ \to J/\psi K^+$	23	*	7	5	**
$B^+ \to J/\psi K^+\pi^+\pi^-$	5	*	2.1	5	**
$\Lambda_b^0 \to J/\psi p K^-$	20	*	0.8	5	**

Table 11: Relative efficiency of the HLT2 selections given the different HLT1 scenarios for the beauty hadrons and quarkonia decay modes. The relative efficiency is defined as the ratio of the number of candidates that are TOS in a given HLT1 scenario to the number of candidates in which any particle(s) in the event satisfies the `VLoose` HLT1 requirements.

Decay mode	`VLoose` (%)	`Loose` (%)	`Tight` (%)	`VTight` (%)
$\Lambda_b^{*0} \to \Lambda_b^0 \pi^+\pi^-$	99	92	87	81
$B^0 \to J/\psi \rho$	99	91	88	79
$B^+ \to J/\psi K^+$	99	80	91	79
$B^+ \to J/\psi K^+\pi^+\pi^-$	100	91	88	79
$\Lambda_b^0 \to J/\psi p K^-$	100	91	85	76

4.5.2 $H_b \to J/\psi X$ decays

Decays of b-hadron of the type $H_b \to J/\psi X$ are fundamental for the LHCb physics programme, and are being used extensively for studies of exotic hadrons, in J/ψ production measurements and as vital control channels for rare decays. The decays studied are $B^0 \to J/\psi \rho$, $B^+ \to J/\psi K^+$, $B^+ \to J/\psi K^+\pi^+\pi^-$ and $\Lambda_b^0 \to J/\psi p K^-$.

The J/ψ candidates are built from pairs of opposite sign muons that are required to form a good quality vertex. The b-hadrons in these decays have a significant lifetime so J/ψ candidates that are detached from the primary vertex are selected. All well reconstructed charged tracks that are inconsistent with originating from the primary vertex and form a good vertex with the J/ψ candidate, are persisted to form b-hadron candidates. Loose particle identification requirements are applied for the muons. The relative efficiency of the different HLT1 selections for each of the decays is shown in Table 11.

The efficiencies, rate and event sizes are detailed in Table 10. The output rate of 0.62 kHz corresponds to bandwidth of 3100 kB/s. In the future this selection will be studied together with the inclusive dimuon trigger described in Section 4.6.8 given the clear overlap between them.

Table 12: Signal efficiency, output rate, expected signal-only rate, event size and bandwidth of the HLT2 rare decays selections for the `VLoose` HLT1 scenario.

Decay mode	Efficiency (%)	Rate (Hz)	Sig. rate (Hz)	Event size (kB)	Bandwidth (kB/s)
$B^0 \to K^{*0}\mu^+\mu^-$	75	13	0.1	7	91
$B^0 \to K^{*0}e^+e^-$	50	500	0.1	5	2500
$B^0 \to K^{*0}\gamma$	6	5	0.8	13	65
$B^0_s \to \phi\gamma$	18	2	0.1	15	30
$B^+ \to K^+\pi^+\pi^-\gamma$	32	13	1	5	65
$\Lambda^0_b \to \Lambda\gamma$	56	60	< 0.1	6	360
$B^0_s \to \mu^+\mu^-$	60	3	< 0.1	4	12
$K^0_S \to \mu^+\mu^-$	20	10	< 0.1	3	30
$\tau^+ \to \mu^+\mu^-\mu^+$	10	30	< 0.1	4	120
Inclusive dimuon	–	1200	–	40	48000
Inclusive dielectron	–	5600	–	40	220000
Inclusive HHγ	–	140	–	4	560
Inclusive HHγ (e^+e^-)	–	90	–	4	360
Inclusive HHHγ	–	140	–	4	560
Inclusive HHHγ (e^+e^-)	–	40	–	4	160

4.6 Rare decays

This section discusses both exclusive and inclusive trigger selections covering all the physics cases under study. The list of modes and a summary of the main results is presented in Table 12. Details on the specific studies are given in the following sub-sections.

4.6.1 $B^0 \to K^{*0}\mu^+\mu^-$

The trigger line developed for $B^0 \to K^{*0}\mu^+\mu^-$ has been produced in three stages. The first step is to implement the current Run 2 preselection in the trigger. This selection is shown in Table 26 in the Appendix, indicated by the non-bracketed numbers. Then a BDT selection is trained using simulated samples with the bracketed requirements in Table 26 applied. The efficiency of this pre-BDT selection on true signal events is 83% for the HLT1 filtered samples, with a minimum bias retention of around 0.5%. The four different HLT1 configurations outlined in Table 1 are investigated prior to training the BDT. The effect of the `Loose` and `Tight` configurations was found to be identical for both signal and minimum bias, effectively giving three different HLT1 configurations. The relative efficiencies for the HLT1 scenarios are given in Table 13.

A BDT was trained for each HLT1 configuration using kinematic and topological variables including the momentum, flight distance, impact parameter and vertex quality of the B^0 candidate and transverse momenta and impact parameters of the other decay products. Picking the BDT point with 90% signal efficiency on the pre-selected events, gives the values shown in Table 12. The expected signal rate is around 0.1 events per second, with an additional two events per second expected for the normalisation channel $B^0 \to J/\psi K^{*0}$. The rate of the presented selection is 13 Hz, and the event size is 7 kB, giving an estimated bandwidth usage of 91 kB/s.

Table 13: Relative Efficiency of the HLT2 $B^0 \to K^{*0}\mu^+\mu^-$ selection given the different HLT1 scenarios. The relative efficiency is defined as the ratio of the number of candidates that are TOS in a given HLT1 scenario to the number of candidates in which any particle(s) in the event satisfies the `VLoose` HLT1 requirements.

Decay mode	`VLoose` (%)	`Loose` (%)	`Tight` (%)	`VTight` (%)
$B^0 \to K^*(892)^0\mu^+\mu^-$	98	90	90	44

4.6.2 $B^0 \to K^{*0}\gamma$ and $B_s^0 \to \phi\gamma$

Photon polarisation in $b \to s\gamma$ transitions can be probed through a time-dependent analysis of $B_s^0 \to \phi\gamma$ decays. On the other hand, $B^0 \to K^{*0}\gamma$ is an important control channel used in most of the radiative analyses. As a starting point, the performance of the Run 2 HLT2 selections for these modes are evaluated in upgrade conditions. However, the rates are seen to be too high (around 1 kHz in both cases) without further optimisation. Therefore, a BDT is developed to improve the background rejection, it is trained and tested using minimum bias and simulated signal samples. The preselection, shown in Table 29 in the Appendix, is based on the current HLT2 selection with some looser cuts to retain enough candidates for the training. The variables used in the BDT are: the impact parameter χ^2 and p_T for the tracks; photon p_T; vertex quality and p_T of the $K^*(\phi)$ candidate; B meson vertex quality, impact parameter χ^2, flight distance χ^2 and p_T.

Following the selection, the signal efficiency is 6% (18%), corresponding to a BDT efficiency of 40% (60%), with an output rate of 5 (2) Hz for $B^0 \to K^{*0}\gamma$ ($B_s^0 \to \phi\gamma$) decays. The event size has been evaluated by adding the flavour tagging information, obtaining an average event size of 13 (15) kB for the $B^0 \to K^{*0}\gamma$ ($B_s^0 \to \phi\gamma$) modes. The corresponding bandwidth results are 65 kB/s for $B^0 \to K^{*0}\gamma$ decays and 30 kB/s for the $B_s^0 \to \phi\gamma$ mode.

4.6.3 $B^+ \to K^+\pi^-\pi^+\gamma$

$B^+ \to K^+\pi^-\pi^+\gamma$ decays permit the study of the helicity structure in electroweak $b \to s\gamma$ transitions through a measurement of the photon polarisation. As a first step, the signal efficiency and bandwidth is estimated for a cut-based preselection similar to the one used in Run 2. In this selection, shown in Table 30 of the Appendix, candidates are built from good quality tracks that are well displaced from the primary vertex. However, this simple selection gives rates of $\mathcal{O}(1\,\text{kHz})$ with a signal efficiency of around 50% using the HLT1 filtered samples. In order to significantly reduce the background rate, a BDT selection inspired from the selection used in the analysis of Run 1 data is applied. The data sets used for the training of the BDT are obtained from the signal and minimum bias upgrade simulation samples. The variables that provide discrimination power are the flight distance χ^2, the impact parameter χ^2 and the flight distance of the B candidate, the quality of the vertex formed by the three-track combination, and the transverse momenta of the reconstructed particles. Several working points are considered, for example a signal efficiency of about 6% can be reached for a rate of 13 Hz. A much lower rate of $\mathcal{O}(0.1$ Hz) can be achieved while keeping the signal efficiency around 2%. Considering the more efficient working point, and an average event size of 5 kB, results in an output bandwidth of 65 kB/s.

4.6.4 $\Lambda_b^0 \to \Lambda\gamma$

This decay mode provides a stringent complementary test of the helicity structure of the electroweak interaction. From the experimental point of view, the reconstruction of this mode is extremely challenging due to the presence of just one long-lived and one neutral particle in the final state, which prevents the Λ_b^0 decay vertex from being reconstructed. Consequently dedicated reconstruction and selection criteria are required to study this mode. Currently unobserved, the branching fraction is expected to be of the same order as for other radiative decays.

Exploiting the upgrade simulation samples, a BDT selection is developed following the strategy used in the Run 2 analysis [16]. This provides a huge improvement in signal to background separation with respect to the results obtained by applying the Run 2 cut-based selection to the same samples, which yield rates of $\mathcal{O}(1\text{ kHz})$ for signal efficiencies of $\mathcal{O}(10\%)$. Separate classifiers are built for candidates reconstructed from long (LL) and downstream (DD) tracks. In the LL case, the chosen cut on the BDT output provides 70% signal efficiency and reduces the minimum bias rate by a factor of 1000 to 60 Hz. These results are summarised in Table 12, and correspond to an output bandwidth of 360 kB/s. A tighter working point gives 50% signal efficiency for a rate of 3 Hz.

The DD case is found to be more challenging due to the reduced momentum resolution, leading to worse discriminating power from the kinematic variables. The proposed working point provides a 25% signal efficiency with a rate of 60 Hz. To reduce the rate further to 6 Hz a signal efficiency of just 5% is necessary. Improvements to the downstream track reconstruction will help to boost performance in this mode.

Further studies on the event size will also be required, to understand persisting all of the necessary information from the calorimeter as well as information on other tracks in the event to determine isolation variables.

4.6.5 $B_s^0 \to \mu^+\mu^-$

The $B_s^0 \to \mu^+\mu^-$ decay is one of the most theoretically clean probes to search for New Physics beyond the Standard Model. Two possible trigger lines are developed for the $B_s^0 \to \mu^+\mu^-$ decay for the upgrade. The first is based on Run 1 and Run 2 analysis preselections and requires two tracks, compatible with the muon hypothesis, forming a secondary vertex well separated from any primary vertex. Additional cuts are applied to the quality of the two tracks and on the invariant mass of the dimuon candidate. The criteria applied are reported in Table 28 in the Appendix and referred to as the *Default Selection*.

The alternative HLT2 selection is developed with the aim to keep the bias on the measurement of the effective lifetime as small as possible. For this reason, requirements on the vertex quality and position of the secondary vertex formed by the two muon candidates are loosened. The reduction of the background rate is achieved by a new muon classifier that exploits the correlation of the hits close to the track extrapolation in the muon detector. The *Alternative Selection* requirements are given in Table 28 in the Appendix.

The results in Table 12 show the performance of the *Default Selection* with about

60% signal efficiency for a rate of just 3 Hz, which corresponds to an output bandwidth of 12 kB/s. The corresponding values for the *Alternative Selection* are 70%, 21 Hz and 84 kb/s for the signal efficiency, rate and bandwidth, respectively. This suggests that tuning the selections further, for example by adding an MVA, can provide better signal efficiency without dramatically increasing the rate.

4.6.6 $K^0_S \to \mu^+\mu^-$

The $K^0_S \to \mu^+\mu^-$ decay is one of the main benchmarks for the study of strange decays at LHCb. The hardware trigger with high p_T requirements in Runs 1 and 2 was the main bottleneck for the study of strange hadrons, which emerge from pp collisions at small angles with respect to the beamline. However, in the LHCb Upgrade, the new software only trigger makes it possible to select this type of decay more efficiently. Large backgrounds are expected from $K^0_S \to \pi^+\pi^-$ and $\Lambda^0 \to p^+\pi^-$ decays, where both final state particles are misidentified. There is also a large component from material interactions.

An HLT2 selection is developed, taking into account the selections used during Run 1 and Run 2. It consists of a set of loose topological requirements on the muons and on the K^0_S candidate, together with tight criteria on the muon identification algorithms, followed by a BDT. The training samples correspond to those discussed in Section 2. The results are shown in Table 12 for the HLT2 selection. The HLT1 efficiency is much lower since currently there is no dedicated HLT1 line to select strange decays.

The performance of this selection largely depends on the muon identification requirements, since these algorithms are not currently optimised for strange decays. The inclusion of tools similar to those in Runs 1 and 2, see Ref. [17], will make the selection more efficient, whilst keeping the $K^0_S \to \pi^+\pi^-$ background under control. Contributions from $\Lambda^0 \to p^+\pi^-$ can be removed by vetoing $\mu^+\mu^-$ candidates with mass hypotheses of p and π applied in a window around the Λ^0 mass , or by applying cuts on the Armenteros-Podolanski plane. Material interactions can also be significantly reduced by the inclusion of new algorithms, as has been proved in Ref. [18].

Currently, the main challenge for the upgrade trigger in $K^0_S \to \mu^+\mu^-$ decays is to reconstruct low transverse momentum particles in HLT1. For this purpose, a dedicated reconstruction algorithm is being developed based on the VELO-TT-Muon matching technique of Run 2 [19]. It has been shown that an inclusive $s \to X\mu\mu$ trigger with the aforementioned improvements reaches an efficiency on filtered events in the 35–50% range for a final output rate of 15–40 Hz, assuming an efficient muon reconstruction is achieved in HLT1 within timing constraints.

4.6.7 $\tau^+ \to \mu^+\mu^-\mu^+$

Lepton flavour violating processes are allowed within the context of the Standard Model with massive neutrinos, but their branching fractions are beyond the reach of any currently conceivable experiment. Observation of charged lepton flavour violation (LFV) would therefore be an unambiguous signature of physics beyond the Standard Model. The search for LFV in τ^- decays at LHCb takes advantage of the large inclusive τ^- production cross-section at the LHC, where τ^- leptons are produced almost entirely from the decays of b and c hadrons. In particular the main source of τ^- leptons is the decay of D^-_s mesons.

In the proposed selection, only two tracks have been requested to be compatible with being muons. This increases the signal efficiency by roughly 20%. For the two tracks with muon compatibility, the output of an MVA discriminant based on the TMVA package [20] is used. It uses the spatial position of the hits in the muon chambers, the timing information of the hits and the crossing of the two views of the muon strips. The results are presented in Table 12, showing a signal efficiency of about 10% for a rate of 30 Hz. This, with the event size, gives the output bandwidth as 120 kB/s.

A better performing muon-identification algorithm using the same input variables but based on CatBoost has been developed, but at the time of writing it was not present in the simulated samples. With these ingredients the rate can be reduced below 30Hz and could be reduced even further with the new MVA discriminant.

4.6.8 Inclusive detached dileptons

An inclusive approach to triggering on a pair of detached dileptons (muons or electrons) is investigated and compared to the exclusive studies shown for $B^0 \to K^*(892)^0\mu^+\mu^-$ and $B^0 \to K^*(892)^0e^+e^-$ decays. The detached dileptons are expected to form a good quality vertex that is well separated from the primary vertex. The leptons are required to be inconsistent with originating from a primary vertex, to be positively identified as a muon or electron as appropriate and to be incompatible with being a ghost track.

Separate multivariate classifiers are used to reduce the backgrounds for the muon and electron lines. Both are trained using upgrade simulation samples and are independently optimised to provide approximately 90% signal efficiency while rejecting more than 90% of the background. The variables used to discriminate between signal and background candidates include the transverse momenta of the detached tracks and their combination, separation of the tracks and vertex from the primary vertex, and the quality of the two or three body vertex. To make the lines as inclusive as possible, all displaced long and downstream tracks are saved, as are π^0 candidates with loose requirements. Optimisation of these requirements to reduce the average event size is postponed to further study, so the event size below should be considered as an upper limit.

The $B^0 \to K^*(892)^0\mu^+\mu^-$ HLT2 signal efficiency for the dimuon line is around 65%, which shows similar performance to the exclusive line described in Section 4.6.1. For the dielectrons, the signal efficiency for $B^0 \to K^*(892)^0e^+e^-$ decays is about 50%, again showing similar performance to the exclusive trigger, as seen in Table 12. The output rate, studied on upgrade minimum bias samples, is about 1.2 kHz (5.6 kHz) for the dimuon (dielectron) lines, as shown in Table 12. With similar average event sizes of around 40 kB, this corresponds to a bandwidth of 48 MB/s (220 MB/s), respectively. The efficiencies for the different HLT1 TOS scenarios are summarised in Table 14. The output rates of the selections fall by roughly a factor of two in the `VTight` case.

These results show that inclusive triggers of this type are feasible for the upgrade trigger; future work will be done to optimise and improve the MVA selections and particle identification requirements for electrons in particular. More detailed studies to understand the event size will also be performed. In addition, similar selections, such as those described in Section 4.5.2, should be studied in parallel and combined if it is appropriate to do so.

Table 14: Relative Efficiency of the HLT2 inclusive dilepton selections given the different HLT1 scenarios. The relative efficiency is defined as the ratio of the number of candidates that are TOS in a given HLT1 scenario to the number of candidates in which any particle(s) in the event satisfies the `VLoose` HLT1 requirements.

Decay mode	`VLoose` (%)	`Loose` (%)	`Tight` (%)	`VTight` (%)
$B^0 \to K^*(892)^0\mu^+\mu^-$	98	94	92	84
$B^0 \to K^*(892)^0e^+e^-$	97	90	88	72

4.6.9 Inclusive radiative trigger

The use of inclusive radiative trigger lines, with a photon in the final state, is seen to be useful to study a variety of $b \to s\gamma$ and $b \to d\gamma$ decays, such as $\Lambda_b^0 \to \Lambda^{*0}\gamma$, $B^0 \to \rho(770)^0\gamma$ or $B^0 \to K_1(1270)^+\gamma$. In particular, the lines are designed to select a final state composed of either two or three hadrons and either a calorimetric or converted photon, resulting in four different trigger lines, one for each possible final state: HHγ, HHγ (e^+e^-), HHHγ and HHHγ (e^+e^-). In addition, extra hadrons are saved to allow for the selection of higher multiplicity decays using the same trigger lines.

These lines exploit common features of radiative decays by applying efficient cuts on kinematic and topological variables, but not on the masses of the reconstructed particles. BDTs are trained for each trigger line, using upgrade simulation samples. In particular, $B^0 \to K^*(892)^0\gamma$, $B_s^0 \to \phi(1020)\gamma$ and $B^0 \to K_1(1270)^+\gamma$ decays are used as the signal proxy for the two-hadron lines and $B^0 \to K_1(1270)^+\gamma$ decays for the three-hadron lines. The minimum bias upgrade simulation sample is used as the background sample for all lines. In addition, the set of variables used in the BDTs has been kept the same as it was in Run 2. Retraining the BDTs increases the signal efficiency and reduces the background rate, compared to using the Run 2 BDTs in upgrade conditions.

The mass of the candidate particles is excluded from the variables used in the BDTs. Instead, the corrected mass of the b-hadron candidate, $m_{corr} = \sqrt{m^2 + p_{\mathrm{T}}{}_{miss}^2} + p_{\mathrm{T}miss}$, is used. This variable allows to efficiently select a final state with up to one missing particle, as its performance degrades with the number of missing particles.

The efficiencies and features of each line are presented in Table 15. The average event size is computed for the four lines together. The bandwidth required by each line is then 560 kB/s (HHγ), 360 kB/s (HHγ (e^+e^-)), 560 kB/s (HHHγ) and 160 kB/s (HHHγ (e^+e^-)). Note these numbers are considered as the lower limit, since the small event size does not yet include the full details of extra persisted tracks or additional calorimeter data that will be required by analysts in Run 3. The different HLT1 configurations are seen to have only a small effect on the signal efficiency, with a typical drop of around 20% between the `VLoose` and `VTight` scenarios.

Finally, the lines also save extra hadrons coming from the same primary vertex, based on some topological cuts. This selection has been tuned using simulated $B^0 \to K_1(1270)^+\gamma$ decays that have passed the HHγ lines, resulting in an 83% efficiency over reconstructible events, while increasing the average event size by only 0.1 kB.

Table 15: Efficiency, rate and event size of each of the radiative inclusive trigger lines with respect to the relevant MC samples.

Line	Decay mode	Efficiency (%)	Rate (Hz)	Event size (kB)
HHγ	$B^0 \to K^*(892)^0\gamma$	13	140	4
	$B_s^0 \to \phi(1020)\gamma$	19		
	$B^0 \to K_1(1270)^+\gamma$	9.3		
HHγ (e^+e^-)	$B^0 \to K^*(892)^0\gamma$	1.1	90	4
	$B_s^0 \to \phi(1020)\gamma$	1.6		
	$B^0 \to K_1(1270)^+\gamma$	1.0		
HHHγ	$B^0 \to K_1(1270)^+\gamma$	8.0	140	4
HHHγ (e^+e^-)	$B^0 \to K_1(1270)^+\gamma$	0.7	40	4

4.7 Inclusive topological trigger

Inclusive b-hadron selections were used successfully during LHCb Run 1 and Run 2, covering the majority of b-hadron decay modes. These "Topological" triggers were designed to select b-hadron decays based on a two-, three- or four-body subset of the decay products, with the full decay chain built offline. A key strength of this strategy is that it allowed a full range of b-hadron decays to be selected, even those not considered until after the data had been collected, allowing the LHCb physics programme to continue to broaden with time. In particular, this kind of inclusive line is essential for studies of semileptonic b-hadron decays, where missing neutrinos ensure that the full decay chain can never be reconstructed. In addition, these selections can be used by a wide range of analyses of hadronic b-hadron decays. This section describes a feasibility study of similar selections for Run 3 conditions.

Inclusive selections based on two- and three-body combinations of detached tracks have been implemented. The four-body selections are left for future work since both the bandwidth and signal efficiency are dominated by two- and three-body selections in Run 2. Two- and three-body combinations of detached tracks are selected, and some loose kinematic and topological requirements are applied to ensure they form a good quality vertex. Multivariate classifiers are then applied separately to candidates from the two- and three-body selections. The classifier is trained to separate between minimum bias and a cocktail of seven signal samples covering the spectrum of b-hadron decays. The variables used to discriminate between signal and background candidates include the transverse momenta of the tracks and the two- or three-body combination, separation of the tracks and vertex from the primary vertex, and the quality of the two- or three-body vertex. The training of the classifier is currently limited by the size of the simulated samples, and a full optimisation of the classifier hyperparameters, so the performance is expected to be a conservative estimate. At a working point giving roughly 75% purity in minimum bias, 75% of signal events containing an initial two-body candidate are selected. This is comparable to the performance of the topological trigger used during Run 2.

To make full use of an inclusive trigger many detector objects outside of the trigger candidate need to be saved, and so the event size is expected to be larger than for an exclusive b-hadron decay selection which does not include flavour tagging. These trigger lines will select a large fraction of the total b-hadron decay spectrum, and are therefore expected to have a high output rate. For this reason the output bandwidth for this strategy is expected to be large. In order to reduce the output bandwidth, the average event size is reduced as much as possible. The advantage of an inclusive trigger is that it can be used for many purposes which were not originally foreseen, this means that care must be taken when considering what additional information is required. It is easy to identify some parts of the event which will not be needed because the majority of tracks are easily assigned to one of the other primary vertices in the event, and these clearly have no relevance to the production or decay of the signal b-hadron. Additional charged tracks therefore are only saved if they originate from the same primary vertex as the signal candidate or if they are strongly detached from any primary vertex, giving an average event size of 35 kB. Adding downstream tracks, those without hits in the vertex detector, and neutral particles adds between 5 to 15 kB to the event size. Three scenarios are considered for the persisted event size, including only additional charged tracks, and extensions to include downstream tracks and also neutral particle information.

The output rate of the topological trigger is found to be 60 kHz, corresponding to a bandwidth of 2.1, 2.4 and 3.0 GB/s for the three event-size scenarios. This compares favourably to the best-case total available upgrade bandwidth of 10 GB/s, and would allow the full physics programme to proceed. For the most pessimistic scenario of 2 GB/s, it is clear that the selection requirements would have to be significantly tighter and choices about the priorities within the physics programme would be required. For the intermediate case of 5 GB/s the full physics programme can be included, though it may rely on some more stringent selection requirements. Nevertheless, this study shows that this approach is feasible in the upgrade regime. Future studies to improve the multivariate classifiers and the persisted event size are expected to give further reductions in the bandwidth requirements. The 50 kB option is considered as the baseline approach because it is the most inclusive approach and provides analysts with the maximum amount of flexibility. Reducing the event size further by removing potentially useful parts of the event will only be considered as a last resort.

4.8 QCD, electroweak and exotica

If dark sector particles are not charged under Standard Model forces, even relatively light dark matter candidates can evade detection in particle physics experiments. Dark photons (A') are a promising candidate for force-mediating particles within the dark-sector. The dark photon can kinetically mix with the Standard Model photon, thereby allowing us to explore this dark sector.

While LHCb will also perform searches for dark photons in the exclusive $D^*(2007)^0 \to D^0(A' \to e^+e^-)$ channel, and inclusive $A' \to e^+e^-$ and prompt $A' \to \mu^+\mu^-$ channels, this analysis focuses on the displaced muonic decay. The dimuon mass range considered is restricted to $214 < A' < 350$MeV. Hence, reconstructing soft muons is paramount. The selection uses kinematic and decay topology requirements, giving a signal efficiency of about 50% for a rate of around 100 Hz for the HLT1 `VLoose` option. With an event size of 3 kB this corresponds to an output bandwidth of 300 kB/s, as shown in Table 16. Note that this event size is a lower limit, future studies to include additional tracks and detached vertices for isolation requirements will increase it. Moving to the `VTight` HLT1 requirements reduces both the signal efficiency and rate by around a factor of two.

Table 16: Signal efficiency, rate, event size and bandwidth of the $A' \to \mu^+\mu^-$ selection.

Decay mode	Efficiency (%)	Rate (Hz)	Sig. rate (Hz)	Event size (kB)	Bandwidth (kB/s)
$A' \to \mu^+\mu^-$	50	100	< 0.1	3	300

5 Conclusion

This note summarises the first round of studies towards the trigger selections required for the LHCb upgrade project, including decays from each corner of the diverse physics programme. Work is underway to ensure optimal performance for strange, charm and beauty decays. Studies of around 30 exclusive trigger lines and six inclusive triggers are presented. The following paragraphs address the aims presented in Section 1.

A summary of the exclusive trigger studies is shown in Table 17. For hadronic b-hadron decays, such as beauty to open charm and charmless beauty decays, the next steps are to compare the performance of the exclusive selections with the topological trigger to decide on the best approach for each group of decay modes. Similarly for those decays including dileptons, from rare decays and charmonia, the inclusive and exclusive approaches must be compared and combined as necessary. For the high-rate charm decays it will be important to study the use of multivariate selections to reduce the output rates. However, extrapolations from the results here suggest that the total charm bandwidth requirements will be manageable. The final selections and choice of working points to tune the efficiencies and bandwidth for each mode are left to future studies.

Studies of the effects of the various HLT1 requirements on the HLT2 selections have been performed, showing up to 50% losses in signal efficiencies between the `VLoose` and `VTight` scenarios for a wide range of the physics programme. The largest effects are seen for charm decays. This provides a clear motivation to ensure that `VLoose` is the baseline choice for HLT1.

The performance of the inclusive triggers is summarised in Table 18. Overlaps between these inclusive selections, in particular those using dimuons will be studied in the future. It will also be important to compare the signal efficiency between inclusive and exclusive approaches for individual channels. The results from the upgrade topological trigger look promising, both in terms of the expected efficiencies and the output rate. The recent LHCb computing TDR [3] states that such a trigger will be used, in at least the first year of the LHCb upgrade, for the majority of the b-hadron physics programme, so work to increase the purity of the selections and to reduce the event size and bandwidth required will be ongoing. Nevertheless, the studies shown here provide confidence that this approach is feasible in the upgrade regime. It should be noted that the inclusion of such inclusive triggers in no way invalidates the exclusive trigger studies for b-hadron decays. The exclusive selections can still be used in HLT2 if required, or will be necessary at a later stage in the offline data processing.

A clear success of the studies presented is the use of multivariate techniques to reduce the backgrounds, and therefore the rates, by up to three orders of magnitude for similar signal efficiencies when compared to the cut-based preselections used in Runs 1 and 2. This demonstrates that it will be important to investigate moving away from cut-based selections and using more advanced methods for the majority of upgrade trigger lines.

Ultimately it is expected that as much of the b-hadron physics programme as possible will move towards the Turbo paradigm, and the numerous studies presented here show the potential to have efficient, exclusive selections with low bandwidth use for a wide range of b-hadron decays modes. The studies here show the event size of a Turbo event will be similar to Run 2. The cost of including tracks for flavour-tagging is around 10 kB per event. For the inclusive approaches, adding all additional tracks and neutral objects from the same primary vertex increases the event-size by about a factor of ten from the typical Turbo event size.

Further studies will follow over the next two years. This will include moving to the new HLT2 selection framework to allow timing studies to be performed. Refinement of the event model may help to reduce the average event sizes, and careful optimisation by analysts will improve the purity and reduce the output rate of the selections. The results so far look promising, but focused effort is required to reach the targets of the project.

Acknowledgements

We express our gratitude to the members of LHCb collaboration for their help in preparing this document, in particular to those who have contributed to the upgrade reconstruction and simulation projects.

References

[1] LHCb collaboration, *Framework TDR for the LHCb Upgrade: Technical Design Report*, CERN-LHCC-2012-007.

[2] LHCb collaboration, *LHCb Trigger and Online Technical Design Report*, CERN-LHCC-2014-016.

[3] LHCb collaboration, *Computing Model of the Upgrade LHCb experiment*, CERN-LHCC-2018-014.

[4] R. Aaij *et al.*, *Tesla: an application for real-time data analysis in High Energy Physics*, Comput. Phys. Commun. **208** (2016) 35, `arXiv:1604.05596`.

[5] R. Aaij *et al.*, *A comprehensive real-time analysis model at the LHCb experiment*, JINST **14** (2019) P04006, `arXiv:1903.01360`.

[6] C. Fitzpatrick *et al.*, *Upgrade trigger: Bandwidth strategy proposal*, Tech. Rep. LHCb-PUB-2017-006. CERN-LHCb-PUB-2017-006, CERN, Geneva, Feb, 2017.

[7] T. Sjöstrand, S. Mrenna, and P. Skands, *A brief introduction to PYTHIA 8.1*, Comput. Phys. Commun. **178** (2008) 852, `arXiv:0710.3820`.

[8] I. Belyaev *et al.*, *Handling of the generation of primary events in Gauss, the LHCb simulation framework*, J. Phys. Conf. Ser. **331** (2011) 032047.

[9] D. J. Lange, *The EvtGen particle decay simulation package*, Nucl. Instrum. Meth. **A462** (2001) 152.

Table 17: The signal efficiency, rate, expected signal rate, event size and bandwidth of the exclusive selections.

Decay mode	Efficiency (%)	Rate (Hz)	Sig. rate (Hz)	Event size (kB)	Bandwidth (kB/s)
$D^{*+} \to D^0(\to K^+K^-)\pi^+$	50	800	1100	6	4800
$D^{*+} \to D^0(\to K^+K^-\pi^+\pi^-)\pi^+$	28	650	310	7	4600
$D^{*+} \to D^0(\to K^0_S\pi^+\pi^-)\pi^+$	19	290	770	7	2000
$D^{*+} \to D^0(\to K^0_S K^+K^-)\pi^+$	14	35	120	7	250
$D^+ \to K^-K^+\pi^+$	49	2700	4800	6	16000
$\Lambda_c^+ \to pK^-\pi^+$	21	5400	11000	6	32000
$D^{*+} \to D^0(\to \pi^+\pi^-\mu^+\mu^-)\pi^+$	38	46	0.2	7	320
$D^{*+} \to D^0(\to e^+\mu^-)\pi^+$	60	220	< 0.1	4	520
$\Xi_{cc}^{++} \to \Lambda_c^+(\to pK^-\pi^+)K^-\pi^+\pi^+$	4	23	0.2	6	140
$B^+ \to D^0(\to K^0_S\pi^+\pi^-)K^+$	20	42	0.2	6	250
$B^0 \to D^+(\to K\pi\pi)D^-(\to K\pi\pi)$	18	10	0.1	16	160
$B^+ \to D^0(\to K^+K^-)K^+$	22	7	0.1	4	28
$B^0_s \to D^+_s(\to KK\pi)K^-$	32	290	0.2	14	4100
$B^+ \to D^0(\to K\pi)K^+\pi^+\pi^-$	17	170	0.9	7	1200
$B^0 \to J/\psi(\to \mu^+\mu^-)K^0_S$	49	20	0.6	15	300
$B^0 \to J/\psi(\to \mu^+\mu^-)\rho^0$	29	21	0.1	5	110
$B^0_s \to J/\psi(\to e^+e^-)\phi$	5	76	1.5	15	1100
$B^0_s \to J/\psi(\to \mu^+\mu^-)\phi$	43	310	2.5	15	4700
$B^0_s \to \phi\phi$	88	190	0.1	18	3400
$\Lambda_b^{*0} \to \Lambda_b^0\pi^+\pi^-$	28	3000	0.2	5	15000
$B^0 \to K^{*0}\mu^+\mu^-$	75	13	0.1	7	91
$B^0 \to K^{*0}e^+e^-$	50	500	0.1	5	2500
$B^0 \to K^{*0}\gamma$	6	5	0.8	13	65
$B^0_s \to \phi\gamma$	18	2	0.1	15	30
$B^+ \to K^+\pi^+\pi^-\gamma$	32	13	1	5	65
$\Lambda_b^0 \to \Lambda\gamma$	56	60	< 0.1	6	360
$B^0_s \to \mu^+\mu^-$	59	3	< 0.1	4	12
$K^0_S \to \mu^+\mu^-$	4	10	< 0.1	3	30
$\tau^+ \to \mu^+\mu^-\mu^+$	10	30	< 0.1	4	120
$A' \to \mu^+\mu^-$	50	100	< 0.1	3	300

[10] P. Golonka and Z. Was, *PHOTOS Monte Carlo: A precision tool for QED corrections in Z and W decays*, Eur. Phys. J. **C45** (2006) 97, `arXiv:hep-ph/0506026`.

[11] Geant4 collaboration, J. Allison *et al.*, *Geant4 developments and applications*, IEEE Trans. Nucl. Sci. **53** (2006) 270; Geant4 collaboration, S. Agostinelli *et al.*, *Geant4: A simulation toolkit*, Nucl. Instrum. Meth. **A506** (2003) 250.

[12] M. Clemencic *et al.*, *The LHCb simulation application, Gauss: Design, evolution and experience*, J. Phys. Conf. Ser. **331** (2011) 032023.

[13] R. Aaij *et al.*, *Upgrade trigger: Biannual performance update*, Tech. Rep. LHCb-PUB-2017-005. CERN-LHCb-PUB-2017-005, CERN, Geneva, Feb, 2017.

Table 18: The rate, event size and bandwidth of the inclusive selections.

Name	Rate (kHz)	Event size (kB)	Bandwidth (MB/s)
Inclusive dimuon	1.2	40	48
Inclusive dielectron	5.6	40	224
$H_b \to J/\psi X$	0.14	5	3.10
Inclusive HHγ	0.23	4	0.92
Inclusive HHHγ	0.18	4	0.72
Topological trigger	60	50	3000

[14] F. Pedregosa *et al.*, *Scikit-learn: Machine Learning in Python*, J. Machine Learning Res. **12** (2011) 2825, arXiv:1201.0490.

[15] S. Benson and K. Gizdov, *NNDrone: a toolkit for the mass application of machine learning in High Energy Physics*, arXiv:1712.09114.

[16] C. Marin Benito and A. Puig Navarro, *Search for $\Lambda_b^0 \to \Lambda^0\gamma$ at LHCb* , .

[17] R. Aaij *et al.*, *Improved limit on the branching fraction of the rare decay $K_S^0 \to \mu^+\mu^-$*, The European Physical Journal C **77** (2017) 678.

[18] LHCb Collaboration, R. Aaij *et al.*, *Search for Dark Photons Produced in* 13 *TeV pp Collisions*, Phys. Rev. Lett. **120** (2018) 061801.

[19] V. Syropoulos, H. G. Raven, and P. Koppenburg, *Controlling Penguins : an estimate of penguin topologies contributing to the weak phase ϕs.*, PhD thesis, 2017, Presented 03 Oct 2017.

[20] A. Hoecker *et al.*, *TMVA 4 — Toolkit for Multivariate Data Analysis. Users Guide.*, arXiv:physics/0703039.

A Appendix

This section contains additional, detailed, information on the selection requirements for some of the studies described previously.

A.1 Beauty to open charm

Table 19 presents the selection criteria for beauty to open charm decay modes. In the table the following definitions are used:

topo-track: $\chi^2_{\rm trk} < 4$ & $p_{\rm T} > 500$ & $p > 5000$;

topo-ks: $p_{\rm T} > 500$ & $p > 5000$ & $\chi^2_{\rm FD}({\rm PV}) > 1000$;

disp-track: $p_{\rm T} > 1700$ & $p > 10000$ & $\chi^2_{\rm trk} < 4$ & $\chi^2_{\rm IP} > 16$ & IP> 0.1mm.

The "BBDT" included in the $B^+ \to D^0(\to K^0_{\rm S}\pi^+\pi^-)K^+$ selection is a generic B hadron BDT which is included in all of the current B2OC stripping lines. Additional variables in table 19 are defined as follows:

- $\chi^2_{\rm vtx}$/ndf - vertex fit quality;
- $\chi^2_{\rm IP}$ - significance of the impact parameter;
- BPVDIRA - cosine of the angle between the B candidate momentum vector and the line connecting the PV and B decay vertex;
- $\chi^2_{\rm FD}(PV)$ - significance of the flight distance with respect to the PV;
- $\chi^2_{\rm trk}$ - quality of the track fit;
- ADOCAMAX - maximum distance of closest approach between the particle decay products;
- ghost prob - the probability that a track is a ghost track (random hits passing the track fit);
- PIDK - particle identification variable to discriminate between kaons and pions;
- BPVVDRHO - cylindrical distance between the particle decay vertex and the PV;
- BPVVDZ - distance between the particle decay vertex and the PV along the beam axis.

A.2 Beauty to charmonia

The selections for the beauty to charmonia decays are given in Table 20 for $B^0 \to J/\psi\,(\to \mu^+\mu^-)\,K^0_{\rm S}(\to \pi^+\pi^-)$ decays, Table 21 for $B^0 \to J/\psi\,(\to \mu^+\mu^-)\,\rho^0)$ decays, Table 22 for $B^0_s \to J/\psi\,(\to e^+e^-)\,\phi$ decays and Table 23 $B^0_s \to J/\psi\,(\to \mu^+\mu^-)\,\phi$ decays. The following variable definitions are used in the above Tables:

- PIDμ - particle identification variable to discriminate between muons and pions;

Table 19: Beauty to open charm selections used for each of the decays. All momenta and masses in MeV.

Target	$B^0 \to D^+(\to K\pi\pi)D^-(\to K\pi\pi)$	$B_s^0 \to D_s^+(\to KK\pi)\pi^-$	$B^+ \to D^0(\to K\pi)K^+\pi^+\pi^-$	$B^+ \to D^0(\to K^+K^-)K^+$	$B^+ \to D^0(\to K_S^0\pi^+\pi^-)K^+$
B	$\sum(p_T) > 5000$ $5000 < M < 6000$ $\chi^2_{vtx}/ndf < 10$ $\tau > 0.2ps$ $\chi^2_{IP} < 25$ BPVDIRA> 0.999 topo-track disp-track* $\Delta_z(D) > -1.5mm$	$\sum(p_T) > 5000$ $4750 < M < 7000$ $\chi^2_{vtx}/ndf < 10$ $\tau > 0.2ps$ $\chi^2_{IP} < 25$ BPVDIRA> 0.999 topo-track disp-track	$\sum(p_T) > 5000$ $5000 < M < 6000$ $\chi^2_{vtx}/ndf < 10$ $\tau > 0.2ps$ $\chi^2_{IP} < 25$ BPVDIRA> 0.999 topo-track disp-track $\Delta_z(D) > 0mm$	$\sum(p_T) > 5000$ $4900 < M < 6500$ $\chi^2_{vtx}/ndf < 10$ $\tau > 0.2ps$ $\chi^2_{IP} < 25$ BPVDIRA> 0.999 topo-track disp-track	$\sum(p_T) > 5000$ $4750 < M < 7000$ $\chi^2_{vtx}/ndf < 10$ $\tau > 0.2ps$ $\chi^2_{IP} < 25$ BPVDIRA> 0.999 topo-track—topo-ks disp-track BBDT> 0.05 $\Delta_z(D) > 0mm$
D	$\sum(p_T) > 1800$ $1834.84 < M < 1904.84$ topo-track $\chi^2_{vtx}/ndf < 10$ $\chi^2_{FD}(PV) > 36$ BPVDIRA> 0 $ADOCAMAX < 0.5\,mm$	$\sum(p_T) > 1800$ $1868.34 < M < 2068.34$ topo-track $\chi^2_{vtx}/ndf < 10$ $\chi^2_{FD}(PV) > 36$ BPVDIRA> 0 $ADOCAMAX < 0.5\,mm$	$\sum(p_T) > 1800$ $1794.84 < M < 1934.84$ topo-track $\chi^2_{vtx}/ndf < 10$ $\chi^2_{FD}(PV) > 36$ BPVDIRA> 0 $ADOCAMAX < 0.5\,mm$	$\sum(p_T) > 1800$ $1814.84 < M < 1914.84$ topo-track $\chi^2_{vtx}/ndf < 10$ $\chi^2_{FD}(PV) > 36$ BPVDIRA> 0 $ADOCAMAX < 0.5\,mm$	$\sum(p_T) > 1800$ $1764.84 < M < 1964.84$ topo-track—topo-ks $\chi^2_{vtx}/ndf < 10$ $\chi^2_{FD}(PV) > 36$ BPVDIRA> 0
h from D	$\chi^2_{trk} < 3$ $p_T > 100$ $p > 1000$ $\chi^2_{IP} > 4$ ghost prob< 0.4 PIDK> 0(< 10) for K(π)	$\chi^2_{trk} < 3$ $p_T > 100$ $p > 1000$ $\chi^2_{IP} > 4$ ghost prob< 0.4	$\chi^2_{trk} < 4$ $p_T > 100$ $p > 1000$ $\chi^2_{IP} > 4$ ghost prob< 0.4 PIDK> 0(< 3) for K(π)	$\chi^2_{trk} < 4$ $p_T > 100$ $p > 1000$ $\chi^2_{IP} > 4$ ghost prob< 0.4 PIDK> 5	$\chi^2_{trk} < 4$ $p_T > 100$ $p > 1000$ $\chi^2_{IP} > 4$ ghost prob< 0.4 PIDK< 20
h from B		$\chi^2_{trk} < 2.5$ $p_T > 500$ $p > 5000$ $\chi^2_{IP} > 4$ ghost prob< 0.4	$\chi^2_{trk} < 4$ $p_T > 100$ $p > 2000$ $\chi^2_{IP} > 4$ ghost prob< 0.4 PIDK> 0(< 3) for K(π)	$\chi^2_{trk} < 4$ $p_T > 500$ $p > 5000$ $\chi^2_{IP} > 4$ ghost prob< 0.4 PIDK> 5	$\chi^2_{trk} < 4$ $p_T > 500$ $p > 5000$ $\chi^2_{IP} > 4$ ghost prob< 0.4
Others			Comb $K_1(1270)$: $M < 3500$ $\sum(p_T) > 1250$ $ADOCAMAX < 0.4\,mm$ topo-track num($p_T < 300$)¡=1 $\chi^2_{FD}(PV) > 16$ BPVDIRA> 0.98 BPVVDRHO> 0.1mm BPVVDZ> 2mm $\chi^2_{vtx}/ndf < 8$		K_S^0 cuts: $p_T > 250$ $\chi^2_{FD} > 50$ $467 < M < 527$ π from K_S^0 cuts:

Table 20: Selection criteria used to identify $B^0 \to J/\psi K^0_S$ candidates. Numbers in parentheses refer to cuts which are only applied to LL candidates.

Target	Variable	Requirement
B^0	$m_{\mu\mu\pi\pi}$	[5000,5650] MeV/c^2
	χ^2_{vtx}/ndf	< 10
	τ	> 0.2 ps
	χ^2 distance from related PV	> 121
	largest minimum χ^2_{IP}	> 9
J/ψ	$m_{p\pi}$	$m_{J/\psi\,\text{PDG}} \pm 80$ MeV/c^2
	χ^2_{vtx}/ndf	< 16
	ADOCAMAX χ^2	< 20
	largest minimum χ^2_{IP}	> 9
$\mu^{\pm}$	PIDμ	> 0
	p_{T}	> 0.5 GeV
K^0_S	$m_{\pi\pi}$	$m_{K^0_S\text{PDG}} \pm 64(35)$ MeV/c^2
	χ^2_{vtx}/ndf	< 25
	ADOCAMAX χ^2	< 25
$\pi^{\pm}$	p	> 2 GeV/c
	p_{T}	(> 0.25 GeV/c)
	minimum χ^2_{IP}	$> 4(9)$

Table 21: Preselection criteria used to identify $B^0_s \to J/\psi\rho(770)$ candidates.

Target	Variable	Requirement
B^0_s	χ^2_{vtx}/ndf	< 10
	χ^2_{IP}	< 25
	BPVDIRA	> 0.999
J/ψ	χ^2_{vtx}/ndf	< 16
	Mass window	$m_{J/\psi\,\text{PDG}} \pm 80$ MeV/c^2
$\mu^{\pm}$	PIDμ	> 0
	p_{T}	> 500 MeV
$\pi^{\pm}$	p_{T}	> 250 MeV
	χ^2_{IP}	> 4
	PIDK	> -10
$\pi^+\pi^-$	Sum p_{T}	> 900 MeV
	χ^2_{vtx}/ndf	< 16
All tracks	χ^2_{track}/ndf	< 5

- ADOCAMAX χ^2- significance of the distance of closest approach between the particle decay products;

- PIDe - particle identification variable to discriminate between electrons and pions.

Table 22: Selection criteria used to identify $B_s^0 \to J/\psi\,(e^+e^-)\phi$ candidates.

Target	Variable	Stripping	Offline	Tight
B_s^0	m	$\in$[3600, 6000] MeV/c^2	-	-
	$\chi^2_{\rm vtx}$/ndf	<10	-	-
	$\tau_{B_s^0}$	>0.3 ps	-	-
	$\chi^2_{\rm vtx}$	-	-	<20
J/ψ	$\chi^2_{\rm vtx}$/ndf	<15	-	-
	$p_{\rm T}$	-	>400 MeV/c	>2000 MeV/c
	Mass window	$\in$[1700, 3600] MeV/c^2	-	-
$e^{\pm}$	PIDe	>0	-	>4
	$\chi^2_{\rm track}$/ndf	<5	<4	-
	$\chi^2_{\rm IP}$	-	>0	-
	$p_{\rm T}$	>500 MeV/c	-	-
ϕ	$p_{\rm T}$	>1000 MeV/c	-	>1500 MeV/c
	$\chi^2_{\rm vtx}$/ndf	<15	<9	-
	Mass window	$\in$[990, 1050] MeV/c^2	-	-
$K^{\pm}$	PIDK	>-3	>0	-
	$\chi^2_{\rm track}$/ndf	-	<4	-
	$p_{\rm T}$	-	>200 MeV/c	-
	p	-	>2000 MeV/c	-
	ghost prob	-	< 0.5	-

Table 23: Selection criteria used to identify $B_s^0 \to J/\psi\,(\mu^+\mu^-)\phi$ candidates.

Target	Variable	Requirement
B_s^0	Mass window	$\in$ [5150, 5550]MeV/c^2
	$\chi^2_{\rm vtx}$/ndf	< 20
	τ	> 0.2 ps
J/ψ	ADOCAMAX χ^2	< 20
	$\chi^2_{\rm vtx}$/ndf	< 16
	Mass window	$\in$ [3020, 3170] MeV/c^2
$\mu^{\pm}$	PIDμ	> 0
	p_T	> 500 MeV/c
ϕ	ADOCAMAX χ^2	< 30
	p_T	> 500 MeV/c
	Mass window	$\in$ [980, 1050] MeV/c^2
	$\chi^2_{\rm vtx}$/ndf	< 25
$K^{\pm}$	PIDK	> 0
All tracks	$\chi^2_{\rm track}$/ndf	< 5

A.3 Charmless beauty decays

The selection criteria for the $B_s^0 \to \phi\phi$ decay are given in Table 24.

Table 24: Summary of the Stripping selections for the $B_s^0 \to \phi\phi$ decay.

Target	Variable	Requirement
B_s^0	$\chi^2_{\text{vtx}}/\text{ndf}$	< 15
ϕ	p_T	$> 2\,\text{GeV}^2/c^2$
	$\chi^2_{\text{vtx}}/\text{ndf}$	< 15
	Mass Window	< 25 MeV/c^2
	$\phi_1\ p_T \times \phi_2\ p_T$	$> 2\,\text{GeV}^2/c^2$
$K^{\pm}$	p_T	> 400 MeV/c
	χ^2_{IP}	> 2.5
	PIDK	> -5

A.4 Beauty hadrons and quarkonia

The selection requirements for $\Lambda_b^{*0} \to \Lambda_b^0 \pi^+\pi^-$ decays are shown in Table 25. An additional variable is defined as

- PIDp - particle identification variable to discriminate between protons and pions.

A.5 Rare decays

The selection requirements for the $B^0 \to K^{*0}\mu^+\mu^-$ decay mode are given in Tables 26 and for $B^0 \to K^0_S\mu^+\mu^-$ in Table 27. Those for the rare decay $B_s^0 \to \mu^+\mu^-$ are shown in Table 28, for $B^0 \to K^{*0}\gamma$ decays in Table 29 and for $B^+ \to K^+\pi^-\pi^+\gamma$ decays in Table 30. An additional variable is defined as

- χ^2_{VS}- significance of the vertex separation between the production and decay vertices.

Table 25: Selection requirements for the $\Lambda_b^{*0} \to \Lambda_b^0 \pi^+ \pi^-$ decay mode.

Target	Variable	Requirement
Λ_b^{*0}	Mass window	$m_{\Lambda_b^{*0}\text{PDG}} \pm 100\,\text{MeV}/c^2$
	$m(\Lambda_b^0\pi^+\pi^-) - m(\Lambda_c^+\pi)$	$30\,\text{MeV}/c^2$
	$\chi^2_{\text{vtx}}/\text{ndf}$	< 5
Λ_b^0	$\chi^2_{\text{vtx}}/\text{ndf}$	< 10
	$\tau_{\Lambda_b^0}$	> 0.2 ps
	Mass window	5400–5800 MeV/c^2
	χ^2_{IP}	< 25
	BPVDIRA	> 0.999
	disp-track	True
	topo-track	True
Λ_c^+	$\chi^2_{\text{vtx}}/\text{ndf}$	< 10
	BPVDIRA	> 0
	ADOCAMAX	0.5 mm
	$\chi^2_{\text{FD}}(PV)$	> 36
	p	$> 5000\,\text{MeV}/c$
	p_{T}	$> 500\,\text{MeV}/c$
All tracks	χ^2_{trk}	< 4
	p	$1000\,\text{MeV}/c$
	p_{T}	$100\,\text{MeV}/c$
	minimum χ^2_{IP}	> 4
	ghost prob	< 0.4
$\pi^{\pm}$	PIDK	< 3
$K^{\pm}$	PIDK	> 5
$p^{\pm}$	PIDp	> -5

Table 26: The non-bracketed numbers show the original stripping selection for $B^0 \to K^{*0}\mu^+\mu^-$. The bracketed numbers indicate how the selection was loosened when producing simulation samples with which to train the BDT.

Target	Variable	Requirement
B^0	$\chi^2_{\rm IP}$	$< 16(25)$
	Mass window	$4800\,{\rm MeV}/c^2 < M < 7100\,{\rm MeV}/c^2$
	BPVDIRA	$> 0.9999(0.9995)$
	$\chi^2_{\rm FD}$	$> 121(9.0)$
	$\chi^2_{\rm vtx}/{\rm ndf}$	$< 8(25.0)$
K^{*0}	Mass window	$< 6200\,{\rm MeV}/c^2$
	$\chi^2_{\rm vtx}/{\rm ndf}$	$< 12(25)$
	$\chi^2_{\rm FD}$	$> 9(0)$
$\mu^+\mu^-$	$m(\mu^+\mu^-)$	$< 7100\,{\rm MeV}/c^2$
	$\chi^2_{\rm vtx}/{\rm ndf}$	$< 12(25)$
	$\chi^2_{\rm FD}$	$> 9(4)$
All tracks	ghost prob	$< 0.4(0.5)$
	minimum $\chi^2_{\rm IP}$	$> 6(4)$

Table 27: Selection requirements for the $B^0 \to K^0_{\rm S}\mu^+\mu^-$ trigger line.

Particle	Requirement
B^0	$\chi^2_{\rm FD}({\rm PV}) > 100$
	BPVDIRA > 0.9995
	$\chi^2_{\rm IP}$ (PV) < 25
	$\chi^2_{\rm vtx} < 9$
	$\lvert m - m_{B^+}\rvert < 1500\,{\rm MeV}$
$\mu^+\mu^-$	$\chi^2_{\rm FD}({\rm PV}) > 16$
	$\chi^2_{\rm vtx} < 9$
	$m < 5500\,{\rm MeV}$
	$p_T > 0\,{\rm MeV}$
	$\chi^2_{\rm IP}$ (PV) > 0
μ	$\chi^2_{\rm IP}$ (PV) > 9
	$p_T > 300\,{\rm MeV}$
$K^0_{\rm S}$	$p_T > 400\,{\rm MeV}$
	$m < 2600\,{\rm MeV}$
	minimum $\chi^2_{\rm IP} > 9$

Table 28: HLT2 selections for $B_s^0 \to \mu^+\mu^-$ decays. The alternative selection uses the new muon classifier, chi2corr, that profit of the correlation of hits close to the extrapolated track in the muon detector.

Target	Default selection	Alternative selection
Tracks	$\chi^2_{\text{IP}}(PV) > 25$ $\chi^2_{\text{track}} < 4$ ghost prob < 0.4	$\chi^2_{\text{IP}}(PV) > 9$ $p_{\text{T}} > 500\text{MeV}$ chi2corr < 5
$\mu^+\mu^-$	$\lvert m(\mu^+\mu^-) - M^{\text{PDG}}_{B^0_s}\rvert < 1200\,\text{MeV}/c^2$ ADOCAMAX < 0.3mm	$\lvert m(\mu^+\mu^-) - M^{\text{PDG}}_{B^0_s}\rvert < 1000\,\text{MeV}/c^2$
B	IP $\chi^2 < 25$ vertex $\chi^2/ndf < 9$ $\chi^2_{\text{FD}} > 225$ BPVDIRA > 0	$\chi^2_{\text{FD}} > 0$

Table 29: Pre-training selection of $B^0 \to K^{*0}\gamma$ and $B_s^0 \to \phi\gamma$ decays, based on Bd2KstGamma and Bs2PhiGamma Hlt2 lines with some looser cuts(*).

Target	Variable	Requirement
B	$\chi^2_{\text{vtx}}/\text{ndf}$	< 20*
	χ^2_{IP}	< 12
	p_{T}	$> 1500\,\text{MeV}/c$ *
	Mass window	$1000\,\text{MeV}/c^2$
$K^*(\phi)$	$\chi^2_{\text{vtx}}/\text{ndf}$	< 20*
	Mass window	$100(20)\,\text{MeV}/c^2$
All tracks	$\chi^2_{\text{track}}/\text{ndf}$	< 4
	χ^2_{IP}	> 20
	p_{T}	$> 300\,\text{MeV}/c$ *
	p	$> 1000\,\text{MeV}/c$ *
Photon	p_{T}	$> 2000\,\text{MeV}/c$

Table 30: Selection criteria used to identify $B^+ \to K^+\pi^-\pi^+\gamma$ candidates.

Target	Variable	Requirement
B^+	Photon and tracks $\sum p_{\rm T}$	> 3000 MeV
	DIRA	> 0
	$\chi^2_{\rm vtx}$/ndf	< 9
	$\chi^2_{\rm IP}$	< 9
	Mass window	$\in [2400 - 6500]$ MeV/c^2
Three-track	$p_{\rm T}$	> 1000 MeV/c
	$\chi^2_{\rm vtx}$	< 9
	$\chi^2_{\rm VS}$	> 0
	Mass window	$\in [0 - 7900]$ MeV/c^2
All tracks	$p_{\rm T}$	> 300 MeV/c
	p	> 1000 MeV/c
	χ^2/ndf	< 3
	$\chi^2_{\rm IP}$	> 20
	ghost prob	< 0.4
Photon	$E_{\rm T}$	> 2000 MeV
	Neutral vs charged identification	> 0